Available online at www.sciencedirect.com
SCIENCE DIRECT®

Polymer 44 (2003) 4651–4654

polymer

www.elsevier.com/locate/polymer

Effect of intercrystallite straight-chain segments on Young's modulus of gel-spun polyethylene fibers

P.M. Pakhomov[a], Svetlana Khizhnyak[a], H. Reuter[b], V. Galitsyn[c], A. Tshmel[d,*]

[a]*Department of Physico-Chemistry, Tver' State University, 170002 Tver', Russian Federation*
[b]*University Osnabrueck, Barbara str. 7, D-49069 Osnabrueck, Germany*
[c]*Institute of Synthetic Fiber, 170032 Tver', Russian Federation*
[d]*Department of Fracture Physics, Ioffe Physico-Technical Institute, Russian Academy of Sciences, 194021 St. Petersburg, Russian Federation*

Received 31 January 2003; accepted 15 April 2003

Abstract

The tensile stress and Young's modulus of a series of gel-spun polyethylene fibers were measured in parallel to measurements of transverse and longitudinal sizes of crystallites, molecular orientation and straight-chain-segment (SCS) length distribution in order to find the correlation of the mechanical and microstructural characteristics during drawing. The low-frequency-Raman data evidence the predominance of the chain-straining process on the ends of crystallites. As a result, there appears a rigid intermediate substance (rigid amorphous phase (RAP)) between crystal cores and true amorphous phase. The RAP is composed of various-lengths SCS oriented in the fiber axis direction and arranged without longitudinal ordering. The RAP transforms gradually to uniform-length taut-tie molecules (TTM). The Young's modulus correlates to the increase of the RAP in length, but there were no detectable response of the mechanical parameters to the formation of the TTM.

Keywords: Polyethylene; Young's modulus; Low-frequency Raman spectroscopy

1. Introduction

The high drawability of the gel-derived (GD) polymers emerges from a very low-density and mobility [1] of the material between fibrils whose quasi-free slippage provides important value of draw ratio. At the same time, the mechanical properties of gel-spun fibers are predominantly determined by their intrafibrillar structure.

In our previous study [2] performed using the longitudinal acoustic mode (LAM) technique in the Raman spectroscopy, we observed the chain-straightening process in melt crystallized (MC) and GD films and fibers made of ultra-high molecular weight polyethylenes (UHMWPE). In drawn MC samples, the average length of the straight-chain-segments (SCS) grows gradually with the draw ratio increase, thus indicating the molecular ordering in the interface zones between the crystallite cores and the amorphous phase. However, there was not revealed a detectable amount of the SCS linking neighboring crystallites, i.e. TTM, in MC samples. The SCS length distributions calculated from the low-frequency Raman spectra of GD fibers, in contrast, showed the presence of populations of TTM entering consecutively a series of a few crystallites.

This work is to assess the significance of the formation of the TTM for the mechanical properties of GD fibers. The results of the mechanical tests carried out to measure the tensile strength (σ) and Young's modulus (E) were put in comparison to the structural data obtained from the infrared (IR) spectroscopy, wide-angle X-ray scattering (WAXS), and low-frequency Raman scattering measurements of a series of samples with different draw ratio (λ).

2. Experimental

The fiber preforms made of UHMWPE with $M_W = 1.7 \times 10^6$ were formed from paraffin oil solution using a multihole die and directed into a bath filled with a liquid

---

[*] Corresponding author. Tel.: +7-812-3030602; fax: +7-812-2478924.
E-mail address: chmel@mail.ioffe.ru (A. Tshmel).

0032-3861/03/$ - see front matter © 2003 Published by Elsevier Science Ltd.
doi:10.1016/S0032-3861(03)00311-2

paraffin. Then the fibers were drawn up to $\lambda = 31$ in a heated bath; the residual solvent was removed by washing with hexane. The fibers with draw ratios up to 22.8 were oriented at the same temperature (119 °C) in order to obtain samples with identical thickness of the intrafibrillar crystal core. The samples with higher value of λ were drawn at 129 °C but these samples were not used in measurements of the longitudinal size of crystallites.

The mechanical tests were performed on 150 mm pieces of samples with the help of the Instron 1122 machine operating in the tensile mode. Strain rate of tests was 50 mm/s; the Young's modulus was mesured at 2% level of strain.

The WAXS experiments were performed on a STADI P STOE & CIE X-ray diffractometer using a monochromatic $\Lambda = 1.54$ Å radiation. The transverse dimensions of crystallites (L) were calculated using the Debye–Scherrer formula:

$$L = K\Lambda/\beta \cos \Theta_{[200]} \tag{1}$$

where $K = 0.94$ is the constant; β is the peak halfwidth measured in radians; $\Theta_{[200]}$ is the diffraction angle of the peak [200].

The polarized IR transmission spectra in the region of the doublet 720/731 cm^{-1} (not shown) were measured with a Fourier spectrometer Bruker Model Equinox 55. The molecular orientation in the crystalline regions was estimated from the square averaged value of cos ϑ :

$$\cos^2\vartheta = (2 - R)/(2 + R) \tag{2}$$

where ϑ is the angle between the orientation axis of the molecular segment and the axis of fiber, R is the dichroic ratio of the 731 cm^{-1} band that corresponds to the vibrations of CH_2 groups in the crystalline regions. In Eq. (2) it is taken into account that the angle between the segment orientation axis and the dipole transition moment direction is equal to $\pi/2$ for this band.

The Raman spectra were measured on a triple monochromator Spex Model 1401 equipped with a 50 mW He–Ne laser. The spectra were recorded in 90° geometry using XX light polarization, and with the fiber axis collinear to X direction.

The measurements were carried out in the spectral range 5 to 30 cm^{-1} where the longitudinal acoustic vibrations propagating along all-*trans* sequences yield a highly polarized band. The shape of such LAM band is determined by the actual SCS length distribution. The SCS situated in crystalline or amorphous regions (those are crystal-involved or individual all-*trans* sequences) contribute to the LAM band in a similar manner.

The average number fraction of the SCS of length l is given by the distribution function $F(l)$ which corresponds to the Raman intensity of the LAM band, $I_{\mathrm{LAM}}(\nu)$, as [3]:

$$F(l) \propto n(\nu)\nu_l^2 I_{\mathrm{LAM}}(\nu), \tag{3}$$

where ν is the Raman shift measured in cm^{-1}; $n(\nu) = 1 - \exp(-hc\nu/kT)$ is the Boltzmann factor, $\nu_l = (2cl)^{-1}(E/\rho)^{1/2}$ is the frequency of acoustic vibrations localized on SCS of length l; c is the speed of light; ρ is the density; E is the Young's modulus in the chain direction.

The Raman signal in the vicinity of the central line is a sum of the Rayleigh scattering and the LAM band intensity. To exclude the contribution of the former, a portion of central line under the LAM spectrum was approximated with a Lorentz function. The difference between the experimental spectrum, $I(\nu)$, and the approximating Lorentzian, $I_{\mathrm{Lor}}(\nu)$, was taken as the effective intensity I_{LAM} in Eq. (3).

3. Results

The measured mechanical parameters are given in Fig. 1(a) and (b). The strength is roughly proportional to λ throughout the draw ratio range, while the growth of Young's modulus begins, in fact, only at $\lambda \cong 7$.

The result found from the WAXS experiments L versus λ plot is shown in Fig. 1(c). At the initial stage of the preform-to-fiber transformation, the transverse size of the folded crystals increases in the course of rearrangement of the primary crystalline entities to axially oriented fibrillar structure. The further drawing causes a gradual ordering of the crystallites in fibrils with achieving a stable value of L at $\lambda \cong 13$. The absence of the correlation between the dependence of E versus λ and L versus λ is in agreement with the one-dimensional character of the modulus-on-λ dependence pointed out in Refs. [3,4]. It is worth noting that the stabilization of the transverse sizes of crystallites occurs when the molecular orientation in crystalline regions (and consequently, of the crystallites themselves as hard entities) is effectively completed (Fig. 1(d)). The Young's modulus does not correlate to the orientation of crystallites.

The original Raman spectra in the frequency range of the LAM bands are shown in Fig. 2. Each spectrum was corrected for contribution of the central line by fitting an appropriate Lorentzian. Fig. 3 shows an example of the differential Raman spectrum, $I_{\mathrm{LAM}}(\nu) = I(\nu) - I_{\mathrm{Lor}}(\nu)$, obtained in result of this computing procedure applied to the $\lambda = 22.8$ sample. The SCS lengths distributions computed from the differential spectra of this kind are given in Fig. 4 .

When considering the role of SCS in the effect of draw ratio on the Young's modulus, it is instructive to extract from the entire distribution function the λ-independent fraction of the SCS, that is those that belong to folded molecules. Really, the position of the maximum of function $F(l)$ corresponds to the effective longitudinal crystallite size (l_c), that is a sum of the thickness of crystal core (l_{core}) and the length (l_{RAP}) of the SCS which form so-called RAP in the intermediate zone between the crystalline and amorphous regions Fig. 5 :

$$l_c = l_{\mathrm{core}} + l_{\mathrm{RAP}} \tag{4}$$

The position of the maximum of $F(l)$ in the $\lambda = 7.7$ sample

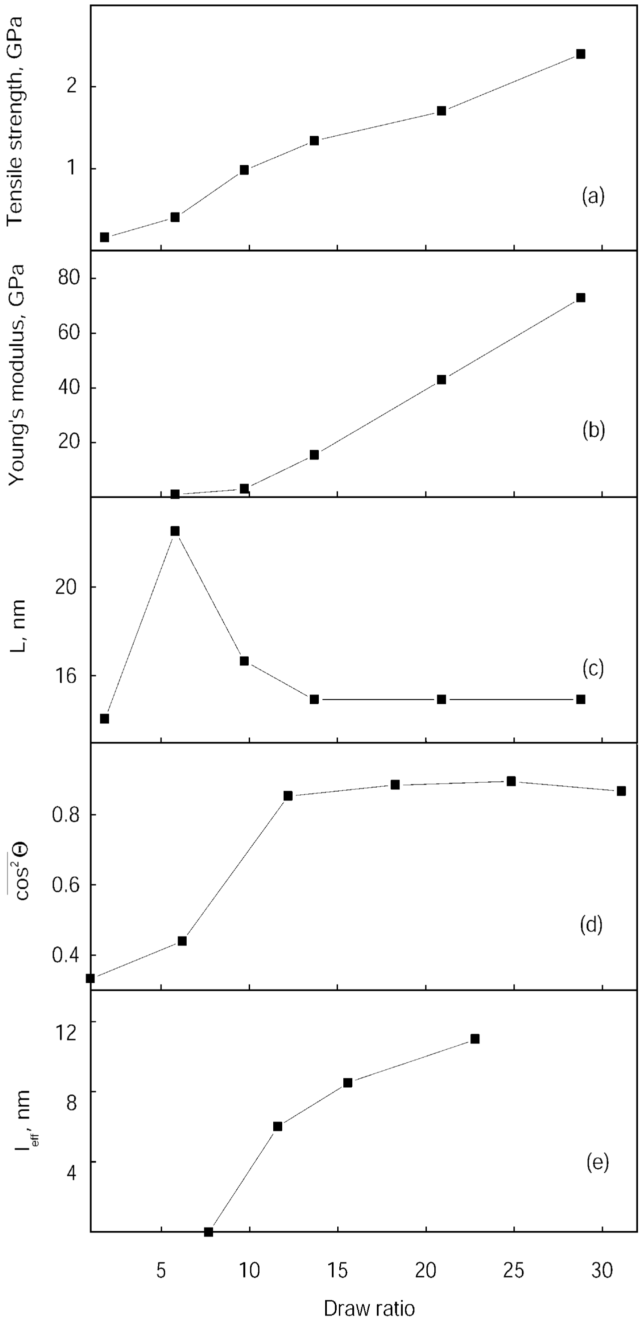

Fig. 1. Mechanical characteristics (a,b), transverse crystal size (c), molecular orientation in crystalline regions (d), and average axial length of intermediate regions (e), in dependence of the fiber draw ratio. Lines serve as a guide for the eyes.

determines, in fact, the value l_{core} since it is justified to suggest $l_{\mathrm{RAP}} \ll l_{\mathrm{core}}$ in this low-oriented sample. The crystal core thickness is independent of the draw ratio in fibers drawn at the same temperature (our experiment is the case). Therefore, one must conclude that the shift of the maximum of $F(l)$ to higher l with the λ increase (Fig. 4) is caused by chain straightening on the ends of crystallites (Fig. 5). This process, that is the RAP formation itself, coincides in its starting points with increase of the Young's modulus (compare Fig. 1(b) and (e)).

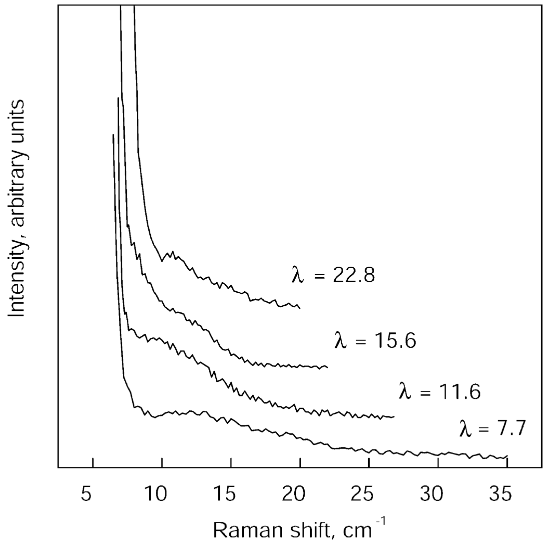

Fig. 2. Low-frequency Raman spectra in the frequency range of the LAM bands. Numbers near spectra denote the draw ratio of samples.

At $\lambda > 15.6$ the distribution function becomes bimodal. The position of the extra peak at 35 nm exceeds $2l_{\mathrm{core}} = 32$ nm where the value of l_{core} was taken from the SCS distribution for the $\lambda = 7.7$ sample (Fig. 2(a)). Consequently, the bimodality means the appearance of the TTM involved in two neighboring crystallites. This qualitative perturbation in the SCS length distribution does not affect a quasi-linear increase of the Young's modulus in the $\lambda > 7.7$ range.

4. Discussion

The increase in the crystal continuity in the fiber axis direction during the hot-drawing procedure results from the chain-straightening process on the ends of folded crystals. The prevailing localization of the chain straightening process in the vicinity of crystallites was previously observed in experiments with the isometric stress relaxation [2]. The effect was explained by the thermodynamical

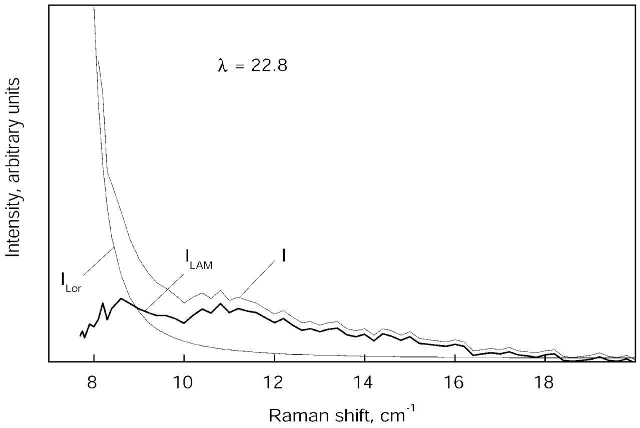

Fig. 3. An example of the spectroscopic data processing: the true LAM intensity results from the subtraction of the Lorentzian-fitted central line from the experimental spectrum.

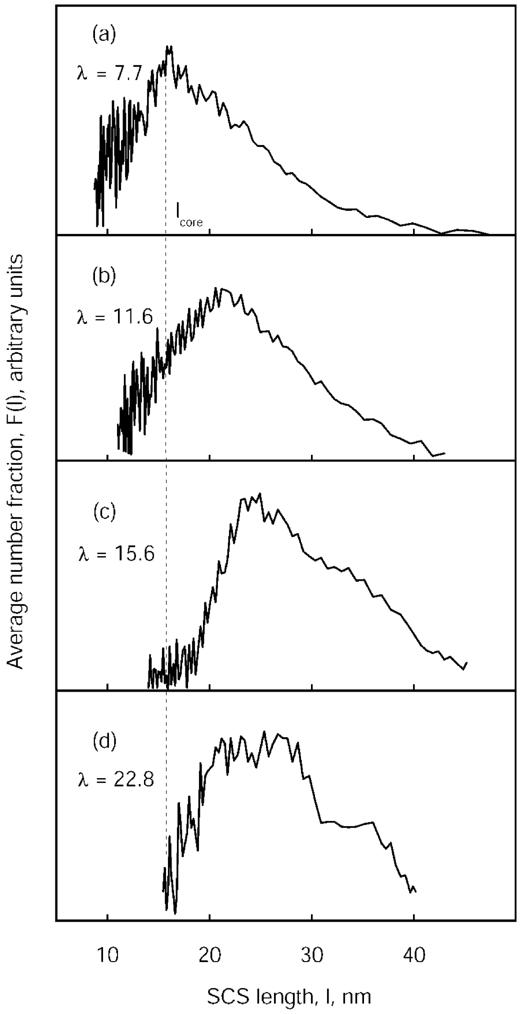

Fig. 4. SCS length distributions in UHMWPE fibers with different draw ratio.

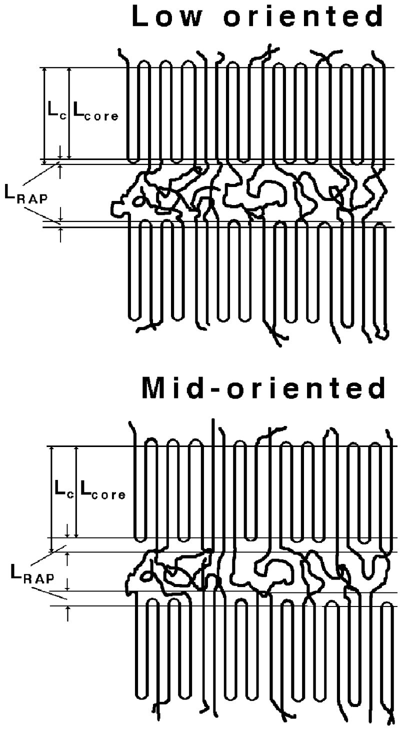

Fig. 5. A schematic model explaining the varying difference between the thickness of the crystallite core and the position of maximum of the distribution function calculated from the LAM data.

profitability of formation of large ordered entities in spite of randomly dispersed individual SCS in the amorphous bulk. The forming intermediate rigid substance is characterized by the parallel arrangement of the SCS and longitudinal disorder. The beginning of persistent growth of the Young's modulus coincides with the appearance of the RAP.

The observation of the longitudinal acoustic vibrations localized on the TTM supports an intercrystallite bridge model [4] used to explain a paradox result emerged from comparison of WAXS and SAXS measurements in highly drawn polyethylenes when the crystalline size in the chain direction occurred to be significantly larger than the long period. This contradiction was resolved by admitting the existence of 'long crystals' linking folded crystallites. The bimodality of the SCS length distribution points out the existence of a particular longitudinal dimension (l_{TTM}) what allows one to suggest belonging of the TTM to quasi-crystalline entities (long crystals). The 'non-crystalline' SCS of length smaller than l_{TTM} and having no longitudinal uniformity form the RAP that could be regarded as a precursor of the crystalline bridges. At the same time, there was not detected any specific response of the Young's modulus on the formation of TTM. Consequently, it is the intercrystallite all-*trans* stems of various lengths, as molecular rigid elements, determine the stiffness of fibrils, while the TTM are nothing but indicators of highly developed ordered structure in the amorphous regions. In the light of the unique relation of the Young's modulus to draw ratio [3–5], this means that the RAP-to-TTM transformation does not break the morphological continuity of the drawing process.

5. Conclusion

In gel-spun fibers made of UHMWPE, the chain-straightening process on the ends of crystallites leads to the development of quasi-ordered structure built of the SCS not involved into folded crystallites. The Young's modulus of the samples correlates with the thickness of the rigid entities measured along the fiber axis.

References

[1] Hu W-G, Schmidt-Rohr K. Polymer 2000;41:2979–87.
[2] Pakhomov PM, Khizhnyak S, Galitsyn V, Ruhl E, Vasil'eva V, Tshmel A. J Macromol Sci-Phys 2002;B41:229–40.
[3] Capaccio G, Wilding MA, Ward IM. J Polym Sci: Polym Phys Ed 1981;19:1489–92.
[4] Al-Hussein M, Davies GR, Ward IM. Polymer 2001;42:3679–86.
[5] Capaccio G, Crompton TA, Ward IM. J Polym Sci: Polym Phys Ed 1976;14:1641–58.